npj | vaccines

Article

Published in partnership with the Sealy Institute for Vaccine Sciences

https://doi.org/10.1038/s41541-025-01314-7

A multivalent capsule vaccine protects against *Klebsiella pneumoniae* bloodstream infections in healthy and immunocompromised mice

Paeton L. Wantuch[1], Lloyd S. Robinson[2], Cory J. Knoot[2], Isra Darwech[2], Aline M. Matsuguma[2], Evgeny Vinogradov[3], Nichollas E. Scott[4], Christian M. Harding[2] & David A. Rosen[1,5] ✉

Klebsiella pneumoniae is a leading cause of nosocomial infections, bacteremia, and worldwide mortality. Further, a drastic rise in antibiotic-resistant isolates poses an urgent threat to humanity. Unfortunately, despite its clinical importance, a licensed *K. pneumoniae* vaccine is not yet available. Here, we report on the production and characterization of the broadest *K. pneumoniae* capsule bioconjugate vaccine to date. We tested this vaccine for its immunogenicity, functionality, efficacy, and antibody durability against a variety of *K. pneumoniae* isolates in a murine bacteremia model. We also established an immunocompromised murine model of bacteremia to better recapitulate human infection and tested our vaccine's efficacy in this background. The tetravalent capsule vaccine is highly immunogenic in mice, generating a robust immune response against all capsule types included (K1, K2, KL102, and KL107). Further, the generated antibodies persist for at least 6 months. The vaccine-induced antibodies are highly functional against a variety of clinical isolates of *K. pneumoniae*, including both classical and hypervirulent strains. Finally, the vaccine led to increased survival after bacteremia challenge compared to placebo-immunized mice. Our findings confirm that a capsule-based bioconjugate vaccine has clinical potential in preventing *K. pneumoniae* infections. These experiments signify much-needed progress towards a multivalent vaccine to combat this increasingly troublesome pathogen.

Klebsiella pneumoniae, a Gram-negative, opportunistic pathogen, is increasingly becoming a global concern. It is responsible for causing a myriad of human diseases in healthy and immunocompromised hosts, as well as in infants and children. Recently, *K. pneumoniae* has been recognized as the most common contributory pathogen in infectious deaths in children under the age of five[1]. Further, *K. pneumoniae* is becoming increasingly difficult to treat given the pathogen's worsening antibiotic resistance profile, often encoding extended-spectrum beta-lactamases (ESBLs) or carbapenemases[2]. In fact, *K. pneumoniae* is the most prevalent of the carbapenem-resistant Enterobacterales[3]. In the United States, multilocus sequence type 258 and 307 (ST258, ST307) strains are endemic high-risk clones often resistant to antibiotics, including third-generation cephalosporins and carbapenems[4]. *K. pneumoniae* can be divided into two major pathotypes, classical or hypervirulent. Classical *K. pneumoniae* (*cKp*) often causes healthcare-associated infections and tends to harbor antibiotic-resistance determinants[5]. Hypervirulent *K. pneumoniae* (*hvKp*) cause community-acquired infections in otherwise healthy hosts and are historically sensitive to most antibiotics[6]; however, recent genetic exchanges with *cKp* isolates have generated *hvKp* isolates with multidrug resistance[7] and *cKp* isolates with hypervirulent genes[8]. Given the upsurge and gravity of antibiotic resistance in *K. pneumoniae*, and the increasing prevalence in *K. pneumoniae* infections globally, additional therapies or preventatives are desperately needed.

[1]Department of Pediatrics, Division of Pediatric Infectious Diseases, Washington University School of Medicine, St. Louis, MO, USA. [2]Omniose, St. Louis, MO, USA. [3]National Research Council Canada, Human Health Therapeutics Centre, Ottawa, ON, Canada. [4]Department of Microbiology and Immunology, The Peter Doherty Institute for Infection and Immunity, University of Melbourne, Parkville, VIC, Australia. [5]Department of Molecular Microbiology, Washington University School of Medicine, St. Louis, MO, USA. ✉e-mail: rosend@wustl.edu

Conjugate vaccines, having been highly successful in combating other bacterial pathogens, are an attractive candidate to target *K. pneumoniae*. Conjugate vaccines are comprised of a polysaccharide of interest covalently attached to a carrier protein to elicit an enhanced adaptive immune response. Two polysaccharides of note are found on the surface of *K. pneumoniae* and have been frequently targeted for vaccine inclusion: the capsular polysaccharide (K-antigen) and the O-antigen polysaccharide of lipopolysaccharide (O-antigen). Conjugate vaccines based on bacterial capsular polysaccharides have successfully diminished the burden of other bacterial diseases and set precedent for a potential *K. pneumoniae* multivalent capsular conjugate vaccine[9,10]. Although *K. pneumoniae* produces over 100 distinct K-types, data from surveillance studies suggest that only 15-20 K-types cause greater than 70% of *K. pneumoniae* infections globally[11,12]. The pneumococcal conjugate vaccine Prevnar is currently formulated with 20 capsular antigens and may soon be broadened to 25-valency[13,14], introducing the feasibility that a high-valent bacterial vaccine is possible.

In this work, we investigate a tetravalent *K. pneumoniae* capsule vaccine as an important stepping stone towards a higher valency vaccine. Importantly, we strategically chose capsule types with high clinical and global importance: K1, K2, KL102, and KL107. The K1 and K2 capsule types account for greater than 80% of *hvKp* isolates[15] and roughly 8% of *cKp* isolates[12,16]. Further, KL107 is highly associated with ST258 strains, while KL102 isolates are associated with ST307. These two sequence types are particularly associated with antibiotic resistance and high-risk clones. A recent study examining a large cohort of *K. pneumoniae* bloodstream isolates found that over 38% expressed either KL102 or KL107 capsule types, which accounted for two out of the top three K-types[4]. Further, K2 and KL102 are among the most prevalent capsule types observed in circulating strains responsible for causing neonatal sepsis in low- and middle-income countries[11]. Together, these data suggest that including these four capsule types would heavily target antibiotic-resistant isolates in addition to hypervirulent strains.

Herein, we describe the production and characterization of a tetravalent capsule bioconjugate vaccine targeting *K. pneumoniae*. Using a variety of *K. pneumoniae* clinical isolates and a murine bacteremia model, we tested the vaccine for immunogenicity, efficacy, and antibody durability. Further, to better mimic the immunocompromised human patients often infected with *cKp*, we established a murine immunocompromised model. This model not only better reflects the human patient population, but it also allows for a lower infecting dose of *cKp* strains required to cause morbidity and mortality. The tetravalent vaccine proved to be highly immunogenic, generating antibodies that persisted for at least six months. The vaccine-induced antibodies were highly functional and led to protection in a lethal murine bacteremia model. Lastly, to our knowledge, the tetravalent vaccine is the broadest *K. pneumoniae* capsule-based conjugate vaccine to date. This study serves as an important step in informing *K. pneumoniae* vaccine design and demonstrates the promising potential of a capsule-based conjugate vaccine targeting *K. pneumoniae*.

Results

Production and authentication of KL102 and KL107 bioconjugate vaccines

To target both hypervirulent and antimicrobial-resistant strains of *K. pneumoniae*, we created a multivalent vaccine that included four major capsular antigens: K1, K2, KL102, and KL107. To produce the KL102 and KL107 *K. pneumoniae* capsular bioconjugates, we cloned the biosynthetic gene clusters for each serotype and co-expressed them along with an engineered *Pseudomonas aeruginosa* Exotoxin A (EPA) carrier protein containing two PglS sequons and the *Acinetobacter baylyi* ADP1 PglS oligosaccharyltransferase in glycoengineered strains of *Escherichia coli*, as was previously described for the K1 and K2 bioconjugates[17,18]. Glycoengineered *E. coli* cell lines heterologously expressing the KL102 or the KL107 capsular polysaccharide attached to their outer surface were structurally validated by comparing their HSQC spectra to the native HSQC spectra originally published for the KL102[19] and KL107[20] polysaccharides extracted from *K. pneumoniae* (Supplementary Figs. 1 and 2). The bioconjugate vaccines (including K1 and K2 vaccines) were subsequently produced in shake flask culture, purified, and protein and polysaccharide content determined prior to the mouse experiments. In addition, the KL102 and KL107 vaccines were analyzed via intact mass spectrometry (MS1), with MS1 spectra showing the expected glycan masses (987 Da for KL102 and 923 Da for KL107) associated with each serotype repeat unit were indeed attached to the EPA carrier protein. Moreover, collision-induced dissociation (CID) MS/MS of trypsin-digested glycopeptides was deployed to confirm the correct glycan composition of the KL102 and KL107 glycans attached to EPA (Supplementary Fig. 3). Lastly, glycosylation events were localized using mass spectrometry electron-transfer/higher-energy collision dissociation (EThcD), again confirming serine 12 of the PglS sequon previously defined by our group (CTGVTQIASGASAATTNVASAQC) was the site of glycosylation (Supplementary Figs. 4–6).

Immunization with K4V yields robust IgG titers

Prior to initiating efficacy testing of the tetravalent vaccine, we performed dose escalation studies in mice. Briefly, we immunized sets of CD-1 outbred mice (males and females) with one of three different tetravalent vaccine (K4V-EPA) formulations containing K1-EPA, K2-EPA, KL102-EPA, and KL107-EPA at polysaccharide concentrations of 0.2, 1.0, or 2.0 μg. All vaccines were formulated with 2% aluminum hydroxide gel as an adjuvant at a 1:9 ratio. All mice were immunized on day 0 and subsequently boosted on days 14 and 28. Serum samples were obtained on days 0, 14, 28, and 42 of the study. We tested the day 42 of each immunization group via ELISA using plates coated with bacteria engineered to express one of the four capsule types on their surface. We noted that the 1.0 μg dose resulted in the highest polysaccharide-specific IgG titers as measured by ELISA. There was no statistically significant difference in IgG titers produced by male versus female mice (Supplementary Fig. 7). The remainder of immunizations were carried out using 1.0 μg of polysaccharide per capsule type in female CD-1 mice.

Next, multiple sets of CD-1 outbred mice were immunized and bled as described above, either with EPA carrier protein alone (control) or the K4V-EPA tetravalent vaccine. Antibody levels were measured using ELISA with plates coated with glycoengineered *E. coli*, each genetically engineered to express a specific *K. pneumoniae* capsular antigen on its surface. As expected, we observed increasing levels of polysaccharide-specific IgG against all four capsule types throughout the experiment (Fig. 1). We further tested the immunized mouse sera by whole cell ELISA against six *K. pneumoniae* clinical isolates (Table 1). We noted significant antibody titers against all strains over the course of the immunizations, with the highest levels of antibody binding against the hv*Kp* isolates (Fig. 2). Lastly, we investigated which IgG subtypes were generated after vaccination with K4V-EPA. Using the glycoengineered bacterial strains to coat ELISA plates, we probed for levels of IgG1, IgG2b, IgG2c, and IgG3 against each of the four capsule types. We noted that immunization resulted in a strong IgG1 response, with only slight levels of IgG2b produced, and virtually no IgG2c or IgG3 observed (Supplementary Fig. 8).

Vaccine-generated antibodies are functional in vitro

After determining that immunization with K4V-EPA generated robust antibody levels against all four capsule types, we investigated whether the antibodies were active in traditional antibody functional assays. Serum bactericidal assays (SBAs) measure the antibodies' ability to trigger the complement cascade, resulting in bacterial killing in the presence of exogenous complement. Opsonophagocytic killing assay (OPKA) also measures antibody-mediated bacterial killing, however, in the presence of phagocytes[21]. We first evaluated antibody functionality using the SBA method. We tested day 42 immunization sera from EPA control- or K4V-EPA-immunized mice for the antibodies' ability to kill the six *K. pneumoniae* clinical strains. We noted significant bacterial killing of all six strains from K4V-EPA serum compared to 100% bacterial survival in the presence

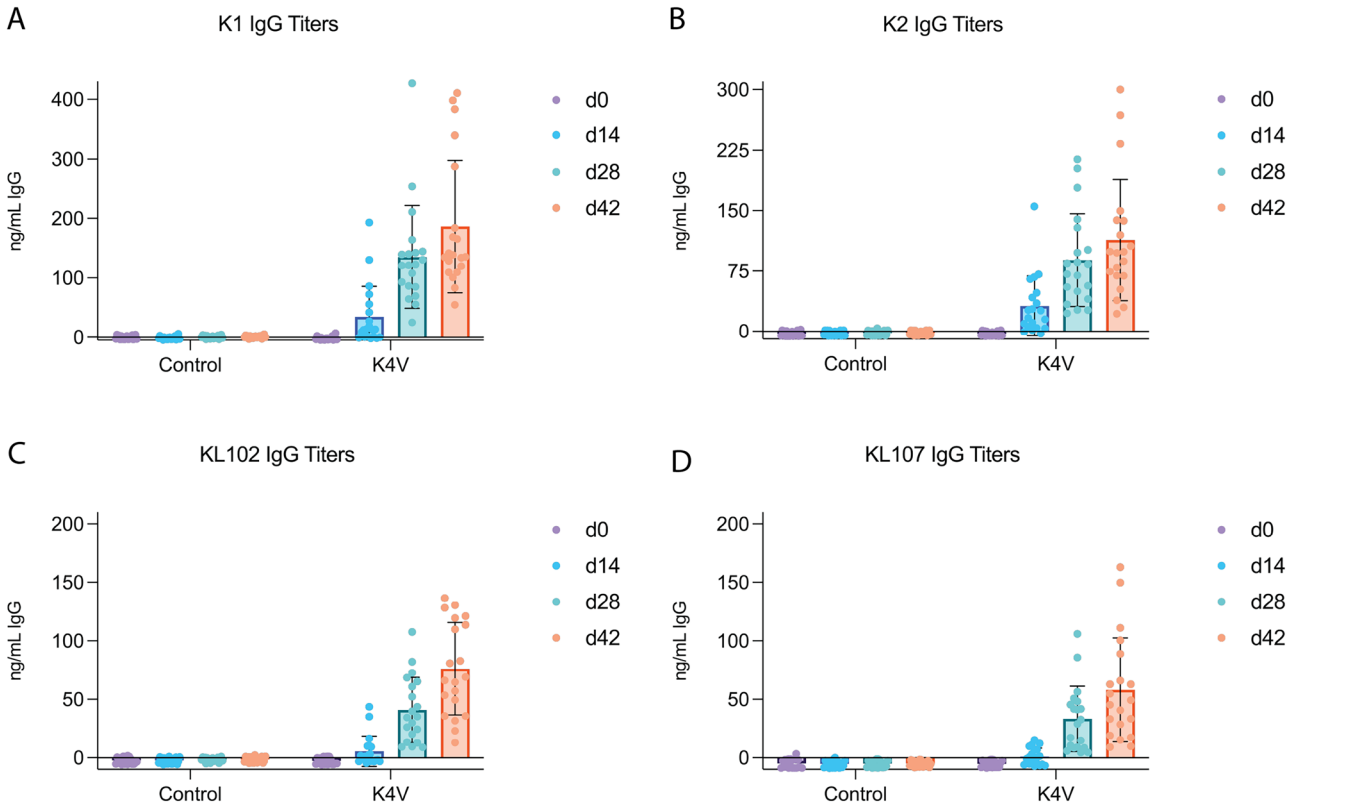

Fig. 1 | Detection of IgG generated by K4V-EPA immunization in mice. Sera from carrier protein alone- (Control) or K4V-immunized mice were used to measure specific IgG concentrations over the course of the immunization series as measured by ELISA against glycoengineered *E. coli* expressing **A** K1 polysaccharide, **B** K2 polysaccharide, **C** KL102 polysaccharide, or **D** KL107 polysaccharide. Graphs display immunoglobulin concentrations of 1:100 serum dilutions as calculated from a standard curve. Error bars represent standard deviation.

Table 1 | *K. pneumoniae* clinical isolates used for infections and assays

Strains	Description	Reference
NTUH-K2044 (hvKp)	Hypervirulent K1 isolate	32
cKp120 (cKp)	Classical K1 isolate (previously referred to as hvKp52)	34
ATCC 43816 (hvKp)	Hypervirulent K2 isolate	31
KR174 (cKp)	Classical K2 isolate	17
BEI 669448 (cKp)	Classical multidrug-resistant KL102 isolate (encodes ESBL and KPC)	33
BEI 702325 (cKp)	Classical multidrug-resistant KL107 isolate	33

of EPA control serum. Vaccine antibodies induced 50-80% complement-mediated bacterial killing of all six strains (Fig. 3).

To perform OPKAs, HL-60 cells were differentiated into a neutrophil-like state as measured by increased levels of CD35 and decreased levels of CD71[22]. Using diluted, heat-inactivated mouse serum, either from control EPA-immunized or K4V-EPA-immunized mice, with baby rabbit complement, we measured the antibodies' ability to induce complement-mediated bacterial killing in the presence or absence of these phagocytes. The K4V vaccine antibodies induced significant bacterial killing by OPKA against all six strains relative to control mouse serum (Fig. 4). Like the SBAs, the most bacterial killing was observed for the K1 capsule-expressing strains NTUH-K2044 (referred to as NTUH) and *cKp*120 (Fig. 4A, B). The other four strains exhibited similar levels of bacterial killing, ranging from 40-65% (Fig. 4C–F). Further, all K1 and K2 strains exhibited increased killing in the presence of phagocytes compared to without. However, BEI 669449 (KL102) and BEI 702325 (KL107) strains did not exhibit increased killing with phagocytes compared to serum and complement alone. Altogether, these data suggest that vaccine-induced antibodies from K4V-EPA immunization are functional in vitro and can induce complement-mediated bacterial killing both in the presence or absence of phagocytes against all matching strains compared to antibodies from control immunized mice, but that addition of phagocytes enhances killing of a subset of these strains.

Determination of vaccine efficacy in a murine model of bacteremia

Given that the K4V-EPA vaccine induces functional antibody production, we sought to test the ability of K4V-EPA to protect mice in a lethal model of bacteremia (Fig. 5). *cKp* isolates each required a relatively high infectious dose to induce mouse lethality, ranging from colony-forming units (CFU) of ~10^7 (BEI 702325) to ~10^9 (BEI 669448), with *cKp*120 and KR174 each requiring a lethal dose of ~10^8 CFU. The *hvKp* isolates NTUH and 43816 were both dosed at 2000 CFU. As previously demonstrated with monovalent formulations of K1-EPA and K2-EPA[17,18], we observed 100% survival of mice challenged with NTUH or 43816 after vaccination with K4V-EPA, compared to complete lethality in control EPA-immunized mice (Fig. 5A, C). The *cKp* isolates resulted in varying levels of protection. There was no significant protection observed in K4V-immunized mice after infection with *cKp*120 or BEI 702325 compared to control-immunized mice (Fig. 5B, F). For isolates KR174 and BEI 669448, we observed modest protection of K4V-EPA-immunized mice compared to controls (Fig. 5D, E). This is consistent with previously published results from a monovalent K2-EPA immunization and challenge with KR174[17]. However, we did note a trend towards protection in K4V-EPA-immunized mice against *cKp* isolates compared to EPA-immunized mice. These data suggest that vaccination with K4V-EPA protects mice from

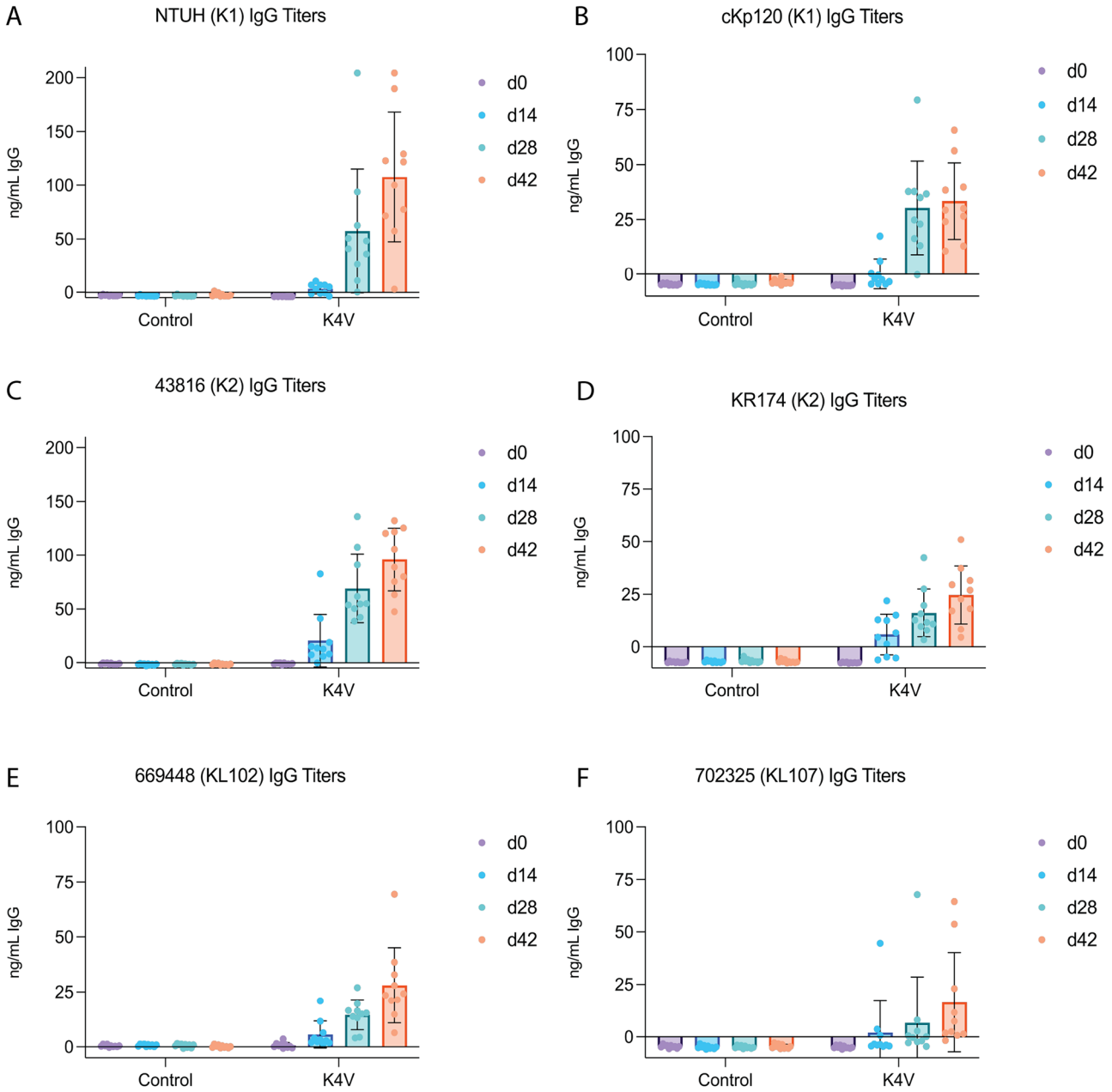

Fig. 2 | *Klebsiella pneumoniae* isolate-specific IgG titers over the course of immunization. Control or K4V-EPA mouse sera were used to measure specific IgG kinetics over the course of the immunization by ELISA against whole bacterial strains: **A** NTUH-K2044, **B** cKp120, **C** ATCC 43816, **D** KR174, **E** BEI 669448, or **F** BEI 702325. Graphs display immunoglobulin concentrations of 1:100 serum dilutions as calculated from a standard curve. Error bars represent standard deviation.

bacteremia with *hvKp* isolates and may also protect mice from some *cKp* isolates.

Establishment of an immunocompromised model of bacteremia to test vaccine efficacy

As noted above, one limitation of the murine *cKp* bacteremia model is the extremely high LD_{90} required for *cKp* infections. Perhaps even the best vaccines would fail in a model in which 10^8 or 10^9 bacteria circulate in the bloodstream of mice. To address this issue, and to better mimic many patients that typically acquire nosocomial bacteremia with *cKp*, we developed a model of bacteremia in a neutropenic host. This model allows for lower inocula of bacteria required to cause disease. Prior to initiation of neutropenia, mice were immunized according to the same timeline as above. At days -4, -1 pre-infection and day +2 post-infection, mice are treated with cyclophosphamide (CPM), an alkylating agent, to induce and maintain an immunocompromised state (Supplementary Fig. 9A). Importantly, complete blood counts were performed on these mice and confirmed a neutropenic state similar to hospitalized immunocompromised patients (Supplementary Fig. 9B). Further, mice were weighed and monitored after treatment with CPM to assess the health of the animals. We observed no fluctuations in weight prior to bacterial infection, corroborating this as a safe method to induce an immunocompromised state in these mice (Supplementary Fig. 9C).

Induction of neutropenia in mice with CPM allowed for the reduction of infectious dose by 1-2 logs for each strain. Indeed, the required lethal doses were reduced to ~5×10^5-10^6 (*cKp*120 and BEI 702325), ~10^7 (KR174), and ~10^8 (BEI 669448). In the immunocompromised model, we observed almost complete protection from *cKp*120 in the K4V-EPA-immunized

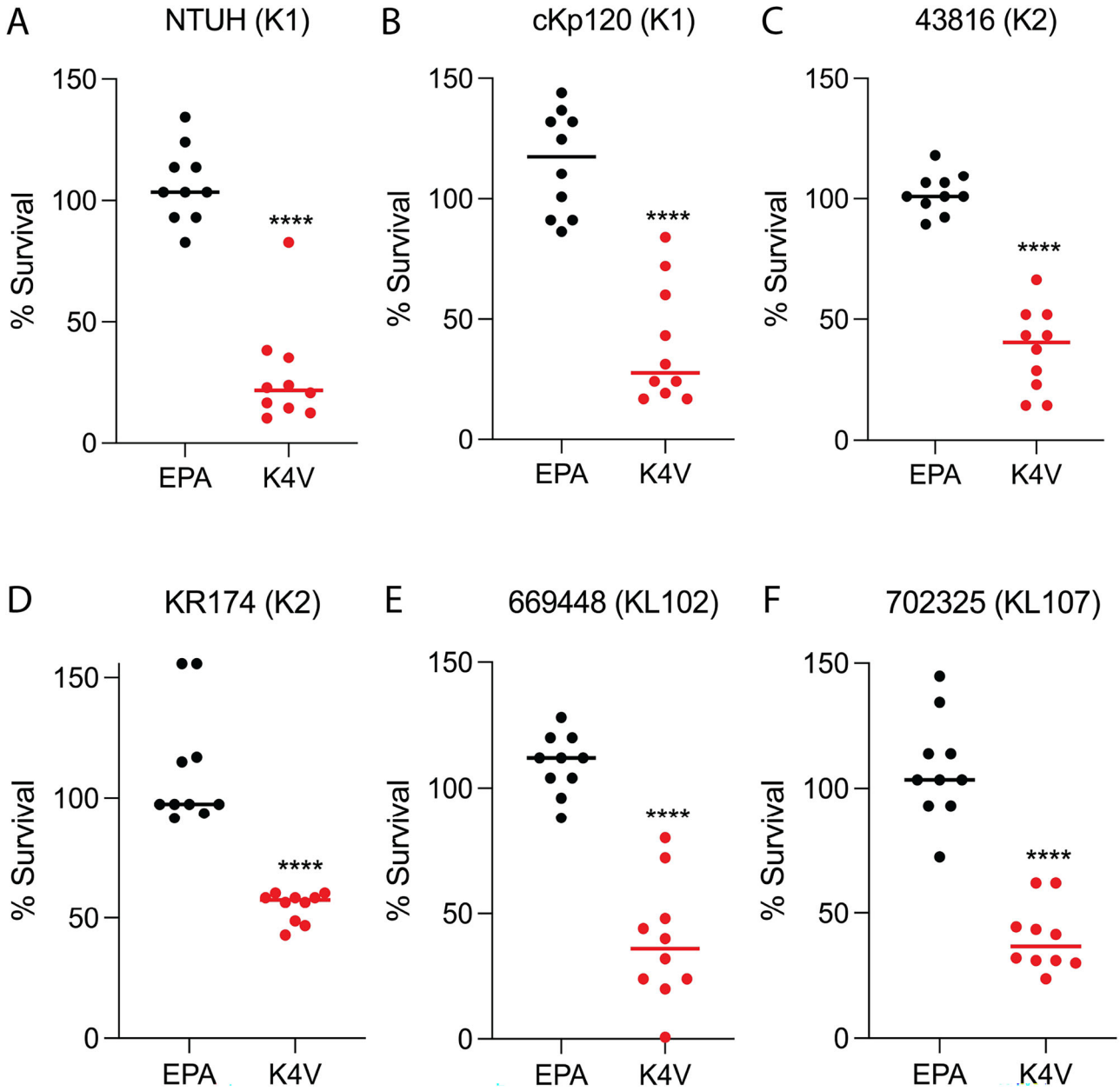

Fig. 3 | Serum bactericidal assays with vaccinated mouse serum. Serum bactericidal assays of day 42 sera from mice immunized with either EPA carrier protein or K4V-EPA bioconjugate vaccines as measured against **A** NTUH-K2044, **B** cKp120, **C** ATCC 43816, **D** KR174, **E** BEI 669448, or **F** BEI 702325. Each data point represents a single mouse. Statistical analyses were performed via Mann-Whitney U test in comparison to EPA survival. Exact p values: ****$p < 0.0001$. Error bars represent standard deviation.

group (Fig. 6A); this contrasts with the immunocompetent bacteremia model in which we observed no significant protection from *cKp*120 using a higher inoculum (Fig. 5B). Likewise, in immunocompromised, K4V-EPA-vaccinated mice, we now observed 80% survival when mice were challenged with the KR174 strain (Fig. 6B). We found 50% survival of K4V-EPA-immunized, immunocompromised mice when challenged with BEI 669448 compared to 0% of control-immunized mice (Fig. 6C). Finally, although modest, we did observe significant survival of K4V-EPA-immunized mice using the immunocompromised model after challenge with BEI 702325 compared to universal death of control-immunized mice. Taken together, these data present an immunocompromised murine model that mimics neutropenic patients and better allows for testing of potential preventatives or therapeutics targeting *K. pneumoniae*. Using this model, we demonstrate that K4V-EPA provides various levels of protection against clinical *K. pneumoniae* isolates.

Vaccine-induced antibodies are functional and protective up to six-months post-vaccination

We have previously demonstrated that the monovalent K2-EPA vaccine induces functional antibodies that were protective and durable for at least six months in mice[23]. To test the ability of the remaining capsule bioconjugates to induce durable and functional immune responses, mice were immunized with each capsule bioconjugate or EPA alone, and serum was collected every month for up to six months. Each of the four vaccines was able to generate robust levels of polysaccharide-specific IgG as measured by ELISA; moreover, these antibodies persisted for at least six months (Supplementary Fig. 10). We also tested whether the six-month antibodies remained functional in vitro and were able to induce bacterial killing. As with the tetravalent formulation, antibodies from each monovalent formulation were able to induce complement-mediated bacterial killing as measured by SBA, even six months post vaccination (Fig. 7). The level of bactericidal activity was

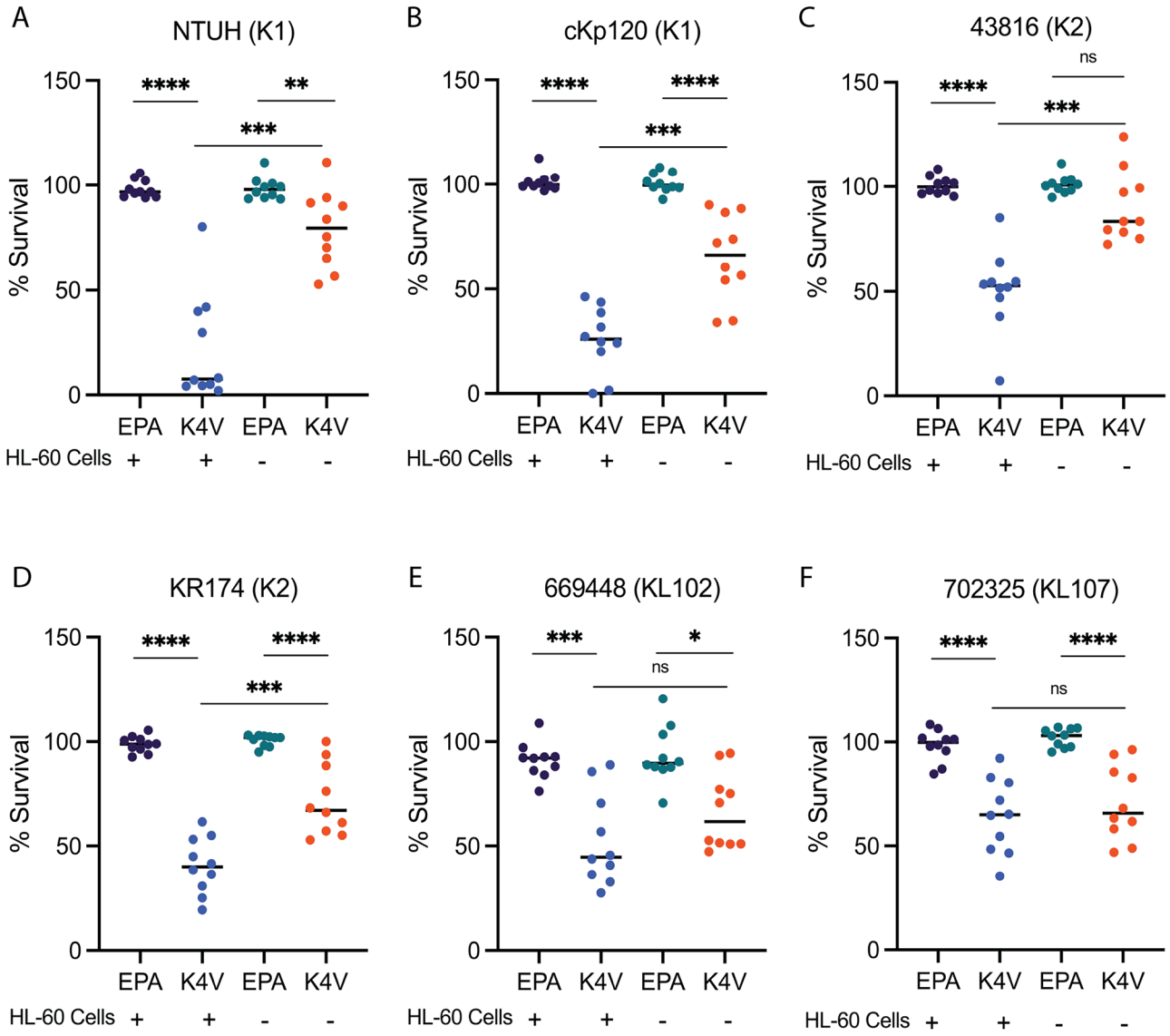

Fig. 4 | Opsonophagocytic killing assay with vaccinated mouse serum. OPKA using day 42 immune serum from mice immunized with EPA carrier protein alone or K4V-EPA bioconjugate vaccines as measured against strains **A** NTUH-K2044, **B** cKp120, **C** ATCC 43816, **D** KR174, **E** BEI 669448, or **F** BEI 702325. As indicated by legend below each graph, bacteria were incubated with combinations of heat-inactivated diluted mouse serum +/− HL-60 cells with baby rabbit complement (BRC). Each data point represents a single mouse. Statistical analyses were performed using Mann-Whitney U tests in comparison to EPA survival or between K4V-EPA groups +/− HL-60 cells. *$p < 0.05$, **$p < 0.01$, ***$p < 0.001$, ****$p < 0.0001$, ns not significant. Error bars represent standard deviation. Exact p values: **A** **** $p < 0.0001$, ** $p = 0.0029$, ***$p = 0.0002$. **B****** $p < 0.0001$, ***$p = 0.0003$. **C** **** $p < 0.0001$, ***$p = 0.0003$, ns $p = 0.0603$. **D** ****$p < 0.0001$, ***$p = 0.0003$. **E** ***$p = 0.0003$, *$p = 0.0115$, ns $p = 0.0753$. **F** ****$p < 0.0001$, ns $p = 0.4813$.

similar for the K1 and K2 expressing strains; however, the percent bacterial killing was slightly lower in KL102 and KL107 antibodies six-month post vaccination (Fig. 7). We then challenged our EPA-control mouse group and our K1-EPA-immunized mouse group with NTUH. Even six-months post-vaccination, we observed 100% survival of K1-EPA mice compared to 0% survival of EPA immunized (Fig. 7). Overall, each monovalent vaccination was able to induce durable antibodies that persisted through at least six-month post-vaccination and maintained their in vitro functionality.

Discussion

K. pneumoniae is a rapidly emerging pathogen that, with increasing rates of antibiotic resistance, is becoming more difficult to treat using conventional methods. Immunization would be an ideal strategy to combat this pathogen; however, there is currently no licensed vaccine. In this present work, we report on the production of a tetravalent capsule bioconjugate vaccine that includes the two most common capsular types associated with hypervirulent isolates (K1 and K2) as well as two of the most prominent capsular types associated with carbapenem resistance in developed countries (KL102 and KL107). We have demonstrated that the tetravalent vaccine produces robust antibodies against all four capsule types that were functional in vitro, leading to complement-mediated bacterial killing. These functional antibodies also translated to in vivo protection in mouse models of bacteremia. Finally, we have developed an immunocompromised bacteremia murine infection model, which allows for better evaluation of potential therapies, especially as they translate to the treatment of neutropenic patients. While all hospitalized patients are susceptible to nosocomial *K. pneumoniae* infections, neutropenic patients are particularly vulnerable to multidrug-resistant infections and carry significantly higher mortality rates[24,25].

One beneficial feature of this neutropenic bacteremia model, beyond better mimicking human populations, is that it allows for better evaluations of treatments or vaccines against classical *K. pneumoniae* strains. Historically, *cKp* strains have been difficult to leverage in animal models as they

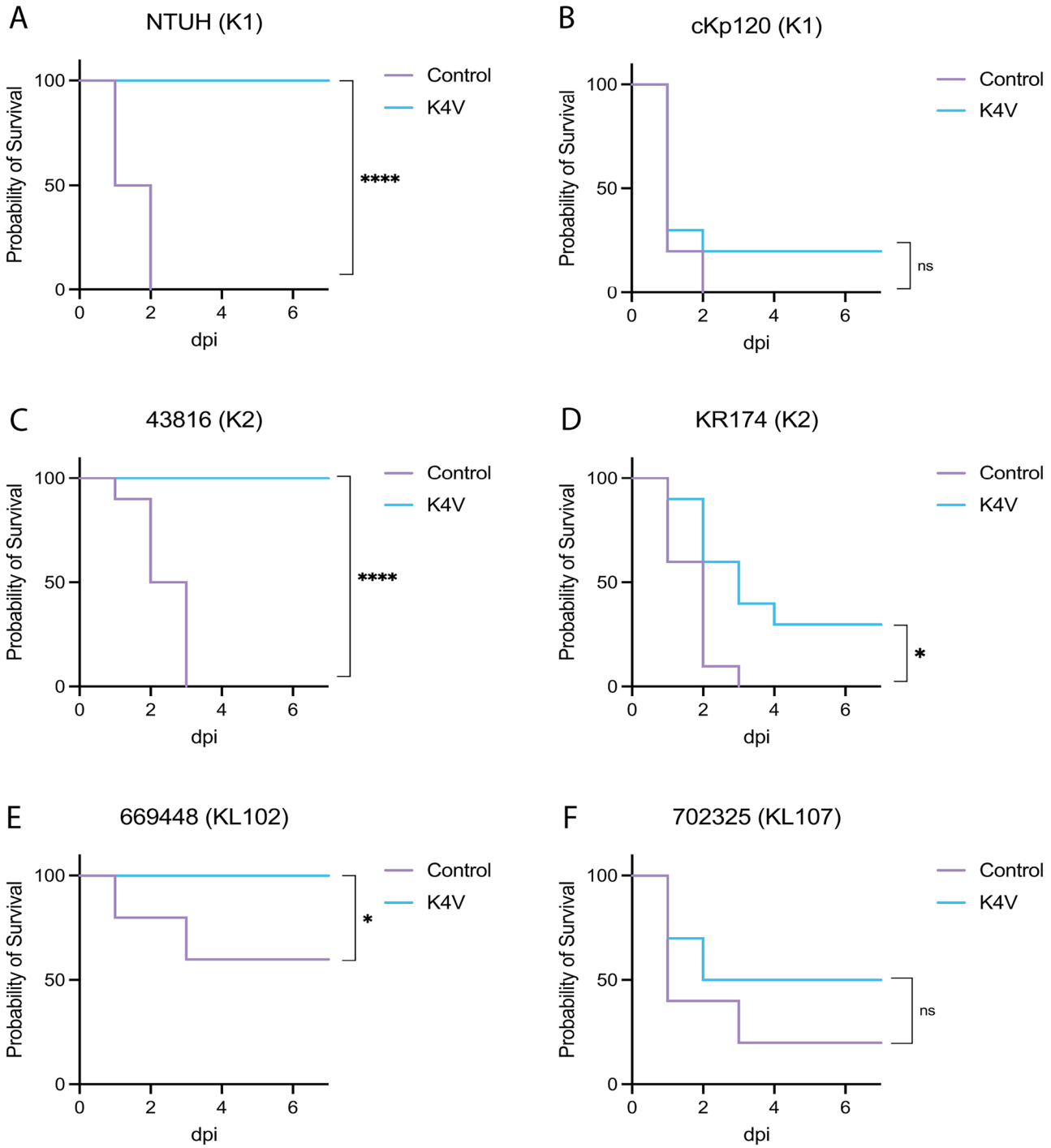

Fig. 5 | Survival of bioconjugate-vaccinated mice after lethal bacteremia challenge. Mice were vaccinated with either the carrier protein EPA alone or K4V-EPA multi-valent capsule vaccine on days 0,14, and 28 followed by intraperitoneal injection with *K. pneumoniae* isolates **A** NTUH-K2044, **B** cKp120, **C** ATCC 43816, **D** KR174, **E** BEI 669448, or **F** BEI 702325. Mice were infected with ~2000 CFU for NTUH and 43816, ~10^7 CFU for BEI 702325, ~10^8 CFU for cKp120 and KR174, and ~10^9 CFU for BEI 669448. Each group contains $n = 10$ mice combined over two independent experiments. Statistical analyses were performed via Log-rank (Mantel-Cox) tests comparing against EPA control group. $^*p < 0.05$, $^{****}p < 0.0001$, ns not significant. Exact p values: **A** ****<0.0001. **B** ns $p = 0.2626$. **C** ****<0.0001. **D** $^*p = 0.0145$. **E** $^*p = 0.0293$. **F** ns $p = 0.1990$.

require an extremely high inoculum to cause infection. We have tackled this challenge by treating mice with CPM prior to infection, effectively making the mice neutropenic. This allowed for lowered infectious doses required to cause disease by as much as two logs for each *K. pneumoniae* clinical isolate. The use of *cKp* strains in healthy mice may not be ideal for evaluating vaccine efficacy between control and vaccinated mice. Certainly, the circulating burden of *K. pneumoniae* required in the traditional bacteremia model is higher than that observed in a typical human bloodstream infection[26]. Utilizing a lower inoculum in neutropenic mice, survival differences can be clearly observed following infection with *cKp* strains that were not seen in healthy mice. Further, protection in the absence of phagocytes provides supporting evidence that prior *K. pneumoniae* vaccination may be effective for immunocompromised, neutropenic patients.

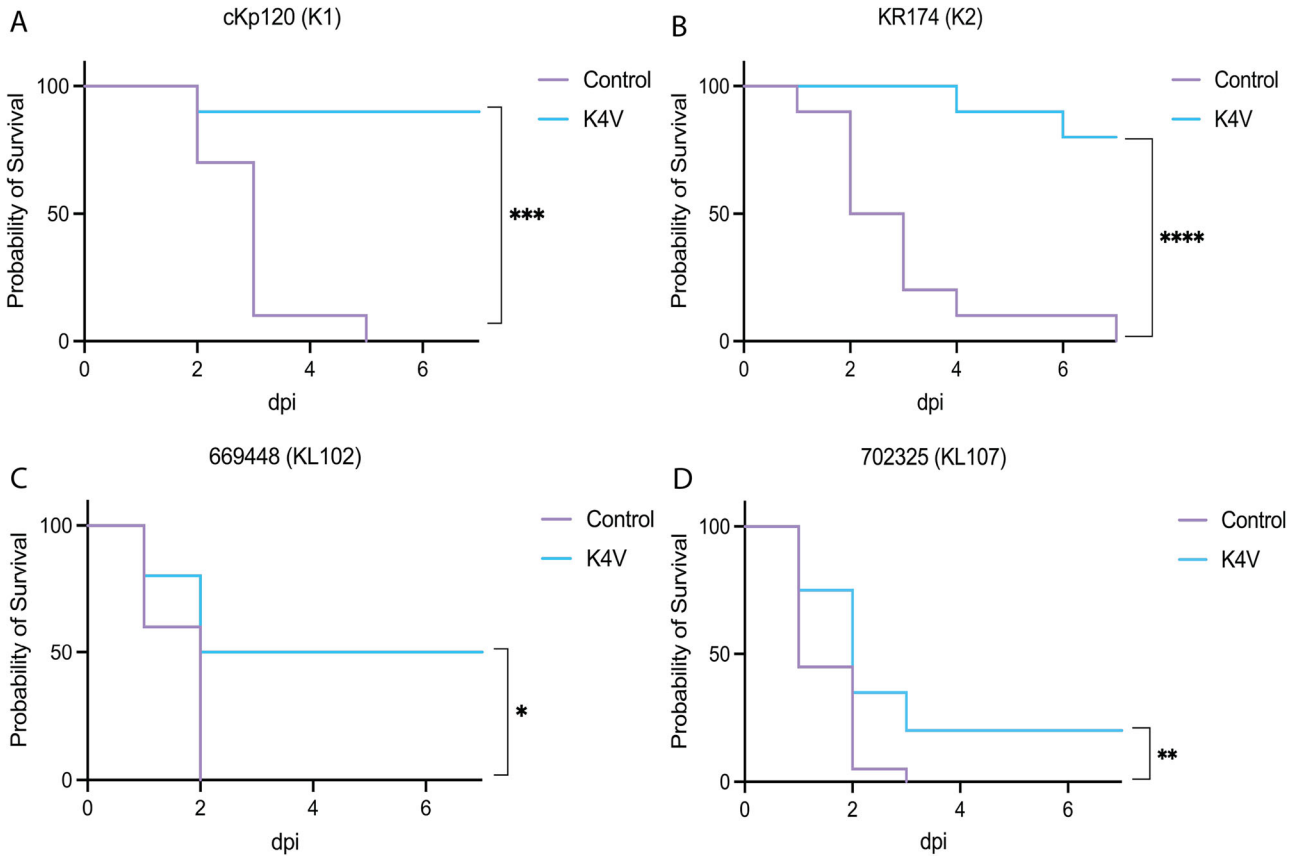

Fig. 6 | Survival of immunocompromised bioconjugate-vaccinated mice after lethal bacteremia challenge. Mice were vaccinated with either the carrier protein EPA alone or the K4V-EPA multi-valent capsule vaccine on days 0,14, and 28. An immunocompromising state was then induced by three injections of cyclophosphamide at 4 days prior to infection (150 mg/kg), one day prior to infection (100 mg/kg), and two days post-infection (100 mg/kg). Mice were then given an intraperitoneal injection with classical *K. pneumoniae* isolates **A** cKp120, **B** KR174, **C** BEI 669448, or **D** BEI 702325. Mice were infected with ~10^6 CFU for cKp120 and BEI 702325, ~10^7 CFU for KR174, ~10^8 CFU for BEI 669448. Each group contains n = 10 mice combined over two independent experiments. Statistical analyses were performed via Log-rank (Mantel-Cox) tests comparing against EPA control group. $^*p < 0.05$, $^{**}p < 0.01$, $^{***}p < 0.001$, $^{****}p < 0.0001$. Exact p values: **A** $^{***}p = 0.0001$. **B** $^{****}p < 0.0001$. **C** $^*p = 0.0245$. **D** $^{**}p = 0.0061$.

As there is no known correlate of immune protection for *K. pneumoniae*, we performed both SBA and OPKA functional studies. It should be noted that the clinical isolates used in this study were relatively resistant to complement-mediated killing alone (without specific antibodies) as complement-susceptible strains are generally avirulent in murine models. K1 and K2 vaccine antibodies both functioned relatively well in inducing complement-mediated antibody killing of matched isolates. In the OPKA, we did observe significantly increased killing in the presence of phagocytes compared to control conditions lacking phagocytes, suggesting at least a component of improved killing when active phagocytes are present. It is important to note that the standardized SBA is different than a standardized OPKA lacking phagocytes. While they both contain relatively the same amounts of serum and complement, the bacteria amount, incubation duration, and temperature conditions differ between assays. Further, in our neutropenic mouse model (which lacks circulating phagocytes), we observed nearly 100% protection from bacteremia with K1 or K2 isolates after vaccination, suggesting these K1 and K2 antibodies are functioning primarily through a complement-mediated method and that this method of killing is sufficient for protection. Phagocytes are clearly not necessary for protection under these conditions. The KL102 and KL107 vaccine antibodies did not demonstrate significant differences by OPKA in bacterial killing in the presence or absence of phagocytes. Further, there was improved survival from bacteremia with each of these strains after vaccination in both the healthy and immunocompromised mouse models. These data suggest that phagocytes are not always required for protection and that vaccination may be efficacious even in neutropenic hosts; however, there may be an added killing effect when neutrophils are present against some strains. These considerations are important in evaluating vaccines and their putative applications, especially as they apply to various immunocompromising conditions.

In addition to providing strong data supporting the use of a multivalent capsule-based vaccine to prevent *K. pneumoniae* infection, additional experiments are required to confirm and explain some of our observations. Collectively, data from this study demonstrated that the current formulations are well-suited for optimal immunogenicity with the K1 and K2 antigens. We noted that both capsule types induced quantitatively more IgG antibodies following vaccination; further, the generated antibodies appeared more functionally potent against matched strains, and the antibodies led to better protection from bacteremia compared to the KL102 and KL107 vaccines. There are many possible explanations for these observations including, but not limited to, the higher quantity of antibodies resulting in better protection, KL102- and KL107-specific formulations requiring modification for better immunogenicity, K1- and K2 isolates producing more capsular antigen, or structural specific differences of KL102 and KL107 resulting in differential antibody binding and function. A higher dose of certain antigens (relative to others) may also be required for similar efficacy. Additionally, there could be genes outside of the capsular locus that could further modify the capsular structure. While there are no known modifications to KL102 or KL107, potential antigen modifications would not occur with exogenous expression in an engineered *E. coli* strain during the bioconjugation process.

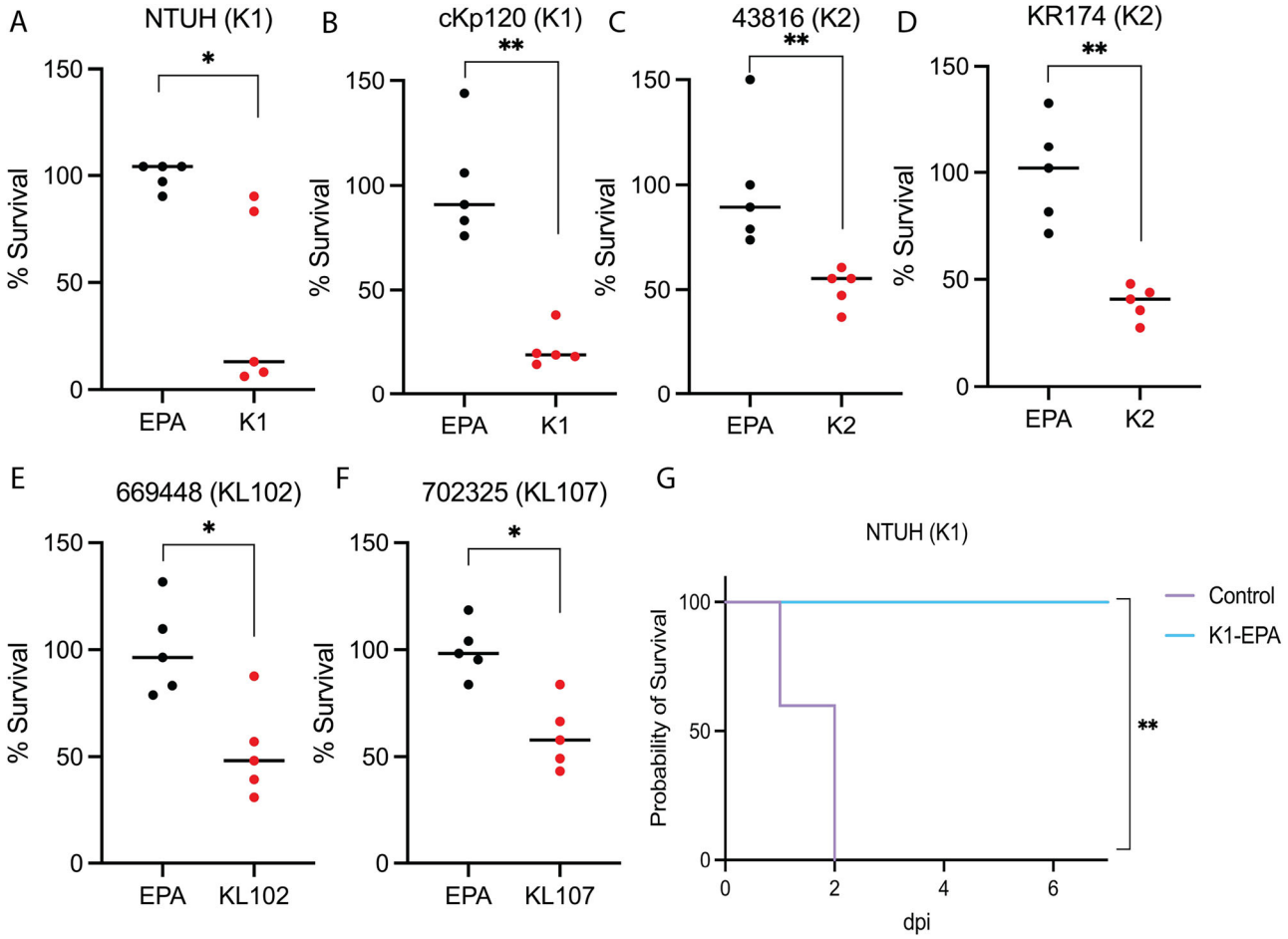

Fig. 7 | Antibody longevity of each bioconjugate vaccine in K4V. Mice were immunized with monovalent formulations of EPA, K1-EPA, K2-EPA, KL102-EPA, or KL107-EPA. Mice were immunized on days 0, 14, and 28 and were bled every month for 6 months. Six-month serums were tested in a serum bactericidal assay against strains **A** NTUH-K2044, **B** cKp120, **C**, ATCC 43816, **D** KR174, **E** BEI 669448, or **F** BEI 702325. After six months, the EPA and K1-EPA immunized cages were challenged intraperitoneally with a lethal dose (~2000 CFU) of NTUH-K2044 and monitored for survival (**G**). Each data point represents a single mouse. Statistical analyses (**A**–**F**) were performed via the Mann-Whitney U test or via (**G**) Log-rank Mantel-Cox test in comparison to EPA survival. $^{*}p < 0.05$, $^{**}p < 0.01$. Error bars represent standard deviation. Exact p values: **A** $^{*}p = 0.0159$. **B** $^{**}p = 0.0079$. **C** $^{**}p = 0.0079$. **D** $^{**}p = 0.0079$. **E** $^{*}p = 0.0317$. **F** $^{*}p = 0.0159$. **G** $^{**}p = 0.0031$.

While this tetravalent capsular bioconjugate *K. pneumoniae* vaccine has promise, these experiments are not without limitations. Four antigens will not be sufficient to cover the majority of pathogenic *K. pneumoniae* strains; current metagenomic studies indicate 15–20 capsular types or more may be necessary[11]. New bioconjugates targeting additional antigens can be engineered, but will each require in vivo and functional studies to assure their efficacy both in isolation and in combination as a component of a multivalent vaccine. Additionally, our group, and others, have explored the possibility of an O-antigen-based conjugate vaccine. There could be protective benefits in combining both O-antigens and K-antigens to target more strains, but this remains uncertain. Indeed, concerns have been raised about capsule masking O-antigen in some strains, suggesting O-antigen alone may not be the best target[17,27–29]. However, as *K. pneumonaie* strains produce a spectrum of capsule quantities, less encapsulated strains may be better targeted by the O-antigen vaccines or protein-based vaccines. The use of a preclinical murine model of bacteremia is also a limitation. While the adaptive immune system of mice is generally similar to that of humans and other mammals, specific differences in immune cells and cytokine signaling imply that murine findings may not always directly translate to human disease[30]. Further, the experiments described here only assess the humoral immune response to vaccination and not potential cell-mediated responses. It is important to continue to study the cell-mediated response as cellular immunity may play a role in vaccine efficacy. It is also critical to test immunizations in other disease models, such as a neonatal sepsis model, to evaluate a putative maternal vaccine.

Overall, these data characterize a tetravalent capsule vaccine targeting *K. pneumoniae* and is an important step towards the development of a broad multivalent vaccine to prevent infections by this troublesome pathogen. Antigens included in this vaccine were particularly chosen for their prevalence in antibiotic-resistant strains; several of the strains used here were multidrug-resistant, suggesting that vaccines may also prove to be an important tool in the global battle against antimicrobial resistance. We demonstrated complement-mediated bacterial killing and in vivo protection from lethal bacteriemia against these strains, highlighting that a conjugate vaccine can protect against antibiotic-resistant isolates. Further, we have established an immunocompromised murine model of bacteremia, a tool that will prove useful in the assessment of future *K. pneumoniae* vaccines, but also in the study of classical *K. pneumoniae* pathogenesis. Overall, this work provides crucial insight that will be leveraged in the ongoing development of an effective multivalent vaccine to target this resistant pathogen.

Methods

Bacterial strains, plasmids, and growth conditions

K. pneumoniae clinical isolates used for infections are listed in Table 1. Additional strains and plasmids used in this study are listed in Supplementary Table 1. *K. pneumoniae* strains were used for all challenge

experiments, ELISAs, and serum bactericidal assays. ATCC 43816 and NTUH- K2044 were previously published and described[31,32]. The pulmonary clinical isolate KR174 was taken from the Rosen Lab clinical *K. pneumoniae* repository and was previously described[17]. Two of the six strains used in this study are part of the BEI Resources Repository *Klebsiella pneumoniae* diversity panel[33]. *cKp*120 was a gracious gift from Thomas Russo and was previously referred to as hvKp52[34]. Primers and oligos used for assembly of DNA constructs in this study are listed in Supplementary Table 2. The *E. coli* VNM47 expression strain was constructed by sequentially deleting the *waaL*, *gtrABS*, and *wecA-yifK* genes from W3110 using Lambda Red-mediated recombination[35]. Finally, the O16 antigen genes *glf-wbbK* were replaced with the *manCB* genes from *K. pneumoniae* ATCC 43816 using gene doctoring[36]. Lambda Red-mediated recombination was also used to construct VNM71. Starting with W3110, the *gtrABS*, *wecA-rffM*, *recA*, and *waaL* genes were sequentially deleted.

Construction of polysaccharide expression plasmids

The K2 two-plasmid expression system was reported previously[17]. Briefly, the K2 locus from *K. pneumoniae* ATCC 43816 was split into two parts using PCR: *wcaJ* to *ugd* were cloned into plasmid pWKS130 to make plasmid pVNM303, and the remaining K2 genes *wcuF* to *wzx* were cloned into plasmid pBBR1MCS3 to make plasmid pVNM299. Splitting the cluster into two plasmids allowed us to produce K2 polysaccharide without co-expressing the transcriptional regulator RmpA[17]. Similarly, for this work, we split the K1 capsule gene cluster from *K. pneumoniae* NTUH-K2044 into two parts. The 3' end of the K1 and K2 clusters encode the same genes[18] and we were able to reuse plasmid pVNM303 for K1 expression. To complete the two-plasmid K1 expression system, we cloned the 5' end of K1 *cps* from genes *wzx* to *wcaI* into plasmid pBBR1MCS3 to make plasmid pVNM340. Co-expression of pVNM303 and pVNM340 afforded K1 capsule synthesis in *E. coli*. The 5' end of the K1 capsule gene cluster (*wzx-wcaI*) was PCR amplified from *K. pneumoniae* NTUH-K2044 genomic DNA using the primer set pWKS-K1 wzx WT RBS F1 and MCS3-K1 wcaI R1. The PCR product was cloned downstream of the *lac* promoter in pBBR1MCS3, resulting in pVNM340. The pVNM379 plasmid was generated by amplifying the KL102 capsule cluster (*wbaP-udg*) from *K. pneumoniae* strain KR32 from the Rosen Lab *Klebsiella* Repository using the primers pWKS-Kp 102 F1 and MCS2-KL102 ugd R1. The PCR product was then inserted into the multiple cloning site of pBBR1MCS2. The KL107 capsule cluster (*wbaP-wzy*) was amplified from *K. pneumoniae* strain AR0362[37] using the primers pWKS-Kp 107 F1 and pWKS-Kp 107 R1. The PCR product was cloned into the KpnI site of pWKS130, resulting in pVNM162.

Production of bioconjugates in E. coli

PglS oligosaccharyltransferase and EPA carrier protein were expressed from plasmid pVNM374 that encodes EPA with 23-amino acid glycosylation sites fused after residues A489 and E548, followed by *pglS* with two amino acid mutations. Both genes were expressed from an IPTG-inducible *tac* promoter. *E. coli* strains were made electrocompetent by pelleting mid-log growth phase culture, followed by two washes with ice-cold 10% glycerol. Cells were spun at 7500 x *g* at 4 °C for 7.5 minutes between washes and stored at −80 °C until use. Plasmid DNA was transformed into 25 µL of cells using a 0.1 cm cuvette and a Bio-Rad Micropulser Electroporator instrument set at 1.8 kV and a 5 ms time constant. Electrocompetent *E. coli* strains VNM47 or VNM71 hosting pVNM374 were electroporated with the polysaccharide expression plasmid(s), outgrown for 1 hour at 37 °C in 1 mL SOC media while shaking, and plated on LB Agar containing Amp 100 µg/mL, Kan 20 µg/mL, and Tet10 µg/mL (for K1 and K2) or Amp100 µg/mL and Kan 20 µg/mL (for KL102 and KL107). 8 – 10 colonies were picked and inoculated into liquid media with requisite antibiotics. The overnight starter was used to inoculate 2 L non-baffled flasks containing 1 L Terrific Broth media (Corning) to a starting $O.D._{600}$ of 0.05. The cultures were shaken at 175 RPM at 30 °C until mid-log when they were induced with 0.1 mM IPTG. K1-producing *E. coli* cultures were dropped to 25 °C after induction; the others were kept at 30 °C. The cultures grew 16–20 hours post-induction and were then harvested by centrifugation at 7500 x *g* for 15 minutes. Pellets were stored at −20 °C until lysis.

Bioconjugate purification and quantitation

Bioconjugates were purified from *E. coli* lysate. Frozen bacterial pellets were resuspended in lysis buffer (20 mM Tris-HCl, pH 8.0, 500 mM NaCl, 10 mM imidazole) containing Pierce protease inhibitor tablets (Fisher Scientific) and 0.5 mM EDTA. Cells were disrupted by two passages through a continuous-flow cell disruptor (Constant Systems) at 35 kpsi, and the lysate was clarified by centrifugation at 18,000 × *g* for 60 minutes. The supernatant containing His-tagged bioconjugates was loaded onto a pre-equilibrated Nickel NTA agarose beads column (GoldBio). The column was washed with equilibration/wash buffer (20 mM Tris-HCl, pH 8.0, 500 mM NaCl, 10 mM imidazole), and proteins were eluted with 300 mM imidazole. The eluate was buffer-exchanged into 20 mM Tris-HCl, pH 8.0, using a 50-kDa cutoff PES centrifugal concentrator (MilliporeSigma), and loaded onto a HiScale Source 15Q anion-exchange column using an ÄKTA pure 25 L FPLC instrument (Cytiva). KL107-EPA and KL102-EPA were purified using a single AEX step, whereas K1-EPA and K2-EPA underwent a second AEX step at lower pH. For all bioconjugates processed at pH 8.0, Buffer A consisted of 20 mM Tris-HCl, pH 8.0, and Buffer B consisted of 20 mM Tris-HCl, pH 8.0, with 1 M NaCl. Proteins were eluted using either a step or linear gradient at a flow rate of 5 mL/minute. For KL107-EPA, proteins were eluted using a step gradient of 5–7.5–10–20% B with 4 column volumes per step; KL107-EPA eluted in the 20% B fractions. For KL102-EPA, proteins were eluted using a linear gradient from 0–30% B over 20 column volumes; KL102-EPA eluted in the 18–21% B fractions. For K1-EPA, a step gradient of 20–40–60% B with 4 column volumes per step was used; K1-EPA eluted in the 40% B fractions. For K2-EPA, a step gradient of 5–10–20–30% B with 4 column volumes per step was used; K2-EPA eluted in the 20% B fractions. Pooled fractions of K1-EPA and K2-EPA were further purified by a second AEX step using a Source 15Q 4.6/100 PE column with lower pH buffers: Buffer A, 20 mM histidine, pH 6.0; and Buffer B, 20 mM histidine, pH 6.0, with 1 M NaCl. For K1-EPA, proteins were eluted using a linear gradient from 5–40% B over 25 column volumes, eluting in the 25–40% B fractions. For K2-EPA, proteins were eluted using a linear gradient from 5–30% B over 20 column volumes, eluting in the 16–24% B fractions. Pooled AEX fractions were concentrated and further purified by size-exclusion chromatography using a HiLoad Superdex 200 16/600 column in 1× TBS buffer at a flow rate of 1.0 mL/minute. Protein concentrations were determined using the Pierce BCA Protein Assay Kit. The polysaccharide content of purified K4V bioconjugates was determined using a modified Anthrone-Sulfuric acid assay[38]. To generate a standard curve, we prepared sugar standards containing mixtures of monosaccharides reflecting the composition of each *K. pneumoniae* capsular polysaccharide based on the reported structures for each of these glycans[18–20]. All monosaccharides used for the standards were purchased from Sigma Aldrich.

Nuclear magnetic resonance (NMR) spectroscopy

The KL102 polysaccharide heterologously expressed in *E. coli* was extracted by heating whole-cell bacteria in 2% acetic acid at 100˚C for 1.5 hours. The insoluble material was removed by centrifugation, and the supernatant, containing a polysaccharide hydrolyzed from the core saccharide of *E. coli*, was subjected to purification on a Bio-Gel P-6 (BioRad) size exclusion chromatography and polished on a ZORBAX C18 (Agilent) column to remove trace protein background. Polysaccharides were dried and analyzed by NMR. The KL107 polysaccharide heterologously expressed in *E. coli* was also extracted by heating whole-cell bacteria in 2% acetic acid at 100 °C for 1.5 hours. The insoluble material was removed by centrifugation, and the supernatant, containing a polysaccharide hydrolyzed from the core saccharide of *E. coli*, was then subjected directly to NMR analysis as the hydrolyzed KL107 polysaccharide extraction was clean. NMR experiments were carried out on a Bruker AVANCE III 600 MHz (1H) spectrometer (25 °C, δ ppm).

Intact Mass Spectrometry

Intact mass analysis was performed on a Xevo G2-XS QTof Quadrupole Time-of-Flight Mass Spectrometer coupled to an ACQUITY H-class UPLC system (Waters) using a Jupiter 300 C5 column (2 mm*50 mm, Phenomenex). Protein samples were resuspended in 20% acetonitrile and loaded directly onto the C5 column at a flow rate of 0.25 mL/minute. Two micrograms of each glycoprotein were desalted on a column for 2 minutes with Buffer A (2% acetonitrile, 0.1% formic acid) before being separated by altering the percentage of Buffer B (80% acetonitrile, 0.1% formic acid) from 0% to 100% over 16.5 minutes. The column was then held at 100% Buffer B for 0.5 minutes before being equilibrated for 1 minute with Buffer A, for a total run time of 20 minutes. Samples were infused into the Xevo G2-XS QTof using electrospray ionization (ESI), and MS1 mass spectra were acquired with a mass range of 400–2000m/z at 1 Hz. Scans across the apex of the elution peaks were summed, peak lists exported before being deconvoluted to identify glycoproteoforms using UniDec[39].

Proteomic Sample Preparation

Glycoproteins were diluted in 10 mM Dithiothreitol (DTT), 100 mM Tetraethylammonium bromide (TEAB), pH 8.5, and reduced for 1 hour at room temperature before being alkylated with 40 mM iodoacetamide in the dark for 1 hour. Alkylation was quenched by the addition of 50 mM DTT for 10 minutes and samples were then digested overnight with 1 µg of Trypsin/Lys-C (1:10 protease: protein) in TEAB pH 8.5 at 37°C. Samples were acidified with Buffer A (2% acetonitrile, 0.01% trifluoroacetic acid) and cleaned up using C18 Stage[40,41] tips to ensure the removal of any particulate matter before being dried by vacuum centrifugation. C18 enriched peptide samples were re-suspended in Buffer A and assessed by LC-MS analysis using a two-column chromatography setup composed of a PepMap100 C18 20-mm by 75-µm trap (Thermo Fisher Scientific) and a PepMap C18 500-mm by 75-µm analytical column (Thermo Fisher Scientific) using a Dionex Ultimate 3000 UPLC (Thermo Fisher Scientific) coupled to an Orbitrap Fusion Lumos Tribrid Mass Spectrometer (Thermo Fisher Scientific). Samples were analyzed using 95-minute runs with samples concentrated onto the trap column at 5 µl/minute for 6 minutes with Buffer A (0.1% formic acid, 2% DMSO) before being separated and infused into the Orbitrap Fusion Lumos at 300 nl/minute via the analytical column. Peptide separation was undertaken by altering the buffer composition from 3% Buffer B (0.1% formic acid, 77.9% acetonitrile, 2% DMSO) to 23% B over 59 minutes, then from 23% B to 40% B over 10 minutes, and then from 40% B to 80% B over 5 minutes. The composition was held at 80% B for 5 minutes before being returned to 3% B for 10 minutes. The Lumos™ Mass Spectrometer was operated in a data-dependent mode, switching between the collection of a single Orbitrap MS scan (450-2000 m/z, maximal injection time of 50 ms, an Automatic Gain Control (AGC) of maximum of $4*10^5$ ions and a resolution of 60k) acquired every 3 seconds followed by three Orbitrap MS/MS scans of the same precursor ion corresponding to a stepped collision energy HCD scan (using NCE 35% with 5% Stepping, maximal injection time of 150 ms, an AGC set to a maximum of $2*10^5$ ions and a resolution of 30k); an Orbitrap EThcD scan (NCE 15%, maximal injection time of 150 ms, AGC set to a maximum of $2*10^5$ ions with a resolution of 30k using the extended mass range setting to improve the detection of high mass glycopeptide fragment ions[40]) and a CID scan (using NCE 35%, maximal injection time of 100 ms, an AGC set to a maximum of $2*10^5$ ions and a resolution of 30k).

Proteomic analysis

Glycopeptides were identified using MSFragger (versions 22.0)[42–44] using the "open searching" option, allowing for potential delta mass on peptides of up to 2000 Da. A tryptic specificity allowing a maximum of two missed cleavage events was set, and Carbamidomethyl was allowed as a fixed modification of Cysteine, while oxidation of Methionine was allowed as a variable modification. A maximum mass precursor tolerance of 20 ppm was allowed at both the MS1 and MS2 levels, with samples searched against an in-house generated protein sequence of EPA. To confirm the identity of glycoforms, spectra were annotated with the aid of the Interactive Peptide Spectral Annotator tool (http://www.interactivepeptidespectralannotator.com/PeptideAnnotator.html)[45]. Raw data files and the associated MSfragger search results have been deposited to the ProteomeXchange Consortium via the PRIDE[46] partner repository with the dataset identifier PXD063900 and are accessible using the login Username: reviewer_pxd063900@ebi.ac.uk and Password: F07o4cW3BCtU.

Murine vaccination

All murine experiments complied with ethical regulations for animal testing and research. Experiments were carried out at Washington University School of Medicine in St. Louis (approved protocol number 23-0300) according to the institutional guidelines and received approval from the Institutional Animal Care and Use Committee at Washington University in St. Louis. Five-week-old male or female CD-1 outbred mice (Charles River Laboratories) were subcutaneously injected with 100 µL of a vaccine formulation on days 0, 14, and 28. The vaccination groups were as follows: EPA carrier protein alone, K1-EPA, K2-EPA, KL102-EPA, and KL107-EPA, or K4V, which is a mixture of all 4 capsule vaccines at 1µg polysaccharide. All vaccines were formulated with Alhydrogel® 2% aluminum hydroxide gel (InvivoGen) at a 1:9 ratio (50 µL vaccine to 5.5 µL adjuvant in 44.5 µL sterile PBS). All vaccination groups received 1 µg of vaccine based on total polysaccharide content. The total polysaccharide content was measured using a modified anthrone-sulfuric assay[38]. Sera were collected on days 0, 14, 28, and 42 prior to immunizations or challenge. Serum was collected from longevity mice on the days previously indicated, as well as once a month for up to six months post the final vaccination. Mice were challenged with either *hvKp* or *cKp* on day 42 (described below).

Enzyme-linked immunosorbent assays

ELISAs were carried out as previously described[17]. Briefly, 96-well plates were coated overnight with specified *K. pneumoniae* or *E. coli* strains in sodium carbonate buffer. After coating, wells were blocked and washed with 0.05% PBS-Tween-20 (PBS-T); all subsequent washes were the same. Sera from immunized mice were diluted 1:100 and added to wells in triplicate, followed by washing, and HRP-conjugated anti-mouse IgG secondary. Plates were washed and developed. Absorbance was determined at 450 nm using a microplate reader (Bio-Tek). Total IgG concentration was determined using an IgG standard curve. All wells were normalized to blank wells coated and treated the same as sample wells without receiving primary mouse sera. Significance was determined using Mann-Whitney nonparametric tests (as not all data were normally distributed per the Shapiro-Wilk test) with $p < 0.05$. All graphs and statistics were generated using GraphPad Prism version 10.

Serum bactericidal assays

Serum bactericidal assays were performed as previously described[17]. *K. pneumoniae* cultures were centrifuged, and the resulting pellets were resuspended in sterile PBS. Cultures were further diluted in sterile PBS to the desired concentration. The assay mixture was prepared in a 96-well U-bottom microtiter plate by combining 70 µL of diluted bacteria and 20 µL of diluted heat-inactivated mouse serum. Day 42 sera from immunized mice were heat-inactivated at 56 °C for 30 minutes. After incubation at 37 °C with shaking for 1 h, 10 µL of baby rabbit complement (Pel-Freez Biologicals) was added to wells at a final concentration of 10% and incubated for an additional 1 h at 37 °C with shaking. Control wells were treated the same as samples except for receiving diluted, heat-inactivated, pre-immune mouse serum. After the final incubation, samples were serially diluted in sterile PBS and plated in pentaplicate. Colonies were counted after 16-h incubation at room temperature. Serum and complement-independent control experiments were performed similarly without specific assay components or with inactivated components. Groups were diluted bacteria in PBS; diluted bacteria with heat-inactivated mouse serum; diluted bacteria with baby rabbit complement; diluted bacteria with heat-inactivated baby rabbit complement. Inactivation of serum and complement controls was achieved

by heating at 56 °C for 30 minutes. Samples were shaken at 37 °C for 2 h, serially titrated in sterile PBS, and plated in pentaplicate. Colonies were counted after 16-h incubation at room temperature. Samples were normalized to percent input, determined as the final bacteria count divided by the starting bacteria count multiplied by 100. Numbers above 100 indicate bacterial growth in the presence of serum during the assay. All graphs and statistics were generated using GraphPad Prism version 10.

Opsonophagocytic Killing Assay (OPKA)

The OPKA methods were adapted from the previously published *Streptococcus pneumoniae* OPKA[47] as well as *K. pneumoniae* OPKA[48]. Human promyelocytic leukemia-60 cell (HL-60 cells) (ATCC) were differentiated into neutrophil-like cells by stimulation with 0.6% N, N-dimethylformamide (DMF) (Sigma-Aldrich) in RPMI-1640 + L-glutamine (Gibco) media supplemented with 10% fetal bovine serum (FBS) for 3 days. The differentiated cells were validated prior to use by flow cytometry; ≥55% in expression of CD35 and ≤20% expression in CD71 in all cells were considered acceptable for the assay[22]. Murine serum was heat-inactivated at 56 °C for 30 minutes and diluted in opsonization buffer (OPB). OPB consists of sterile PBS supplemented with Ca^{+2}/Mg^{+2}, heat-inactivated FBS, and 0.1% sterile gelatin. Working stocks of each bacterium were diluted in OPB to an optimal pre-determined dilution and co-incubated with murine serum in a U-bottom 96-well plate at 37 °C with shaking for 30 minutes. Baby rabbit complement (BRC) (Pel-Freez) was added to a final concentration of 10% and HL-60 cells at a concentration of 10^7/mL were added to each well and incubated at 37 °C with 5% CO_2 for 45 minutes. Controls included carrier protein only immunized mouse serum (EPA) treated under all the same conditions as K4V serum. Additional controls were samples containing no HL-60 cells with serum, plus or minus BRC. Each serum tested had the following conditions: + serum, + BRC, + HL-60; + serum, + BRC, - HL-60; + serum, - BRC, - HL-60. After incubation 50 µL of the reaction mixture was spotted onto an LB agar plate, and CFUs were enumerated the following day after 16 hours of growth. Percent killing was determined as positive test sample conditions, CFU divided by complete negative sample (+serum, -BRC, -HL-60), CFU multiplied by 100. Significance was determined using Mann-Whitney nonparametric tests (as not all data were normally distributed per the Shapiro-Wilk test) with $p < 0.016$ per the Bonferroni correction for multiple comparisons. All graphs and statistics were generated using GraphPad Prism version 10.

Murine challenge experiments and immunocompromised model

All murine immunizations complied with ethical regulations and standards for animal testing as set by the Washington University School of Medicine in St. Louis and the Institutional Animal Care and Use Committee at Washington University in St. Louis. *K. pneumoniae* isolates were administered via intraperitoneal injection for the bacteremia model. Cultures were grown statically in LB broth for 16 h at 37 °C. Cultures were centrifuged at 8000 *x g* for 10 minutes, and pellets were resuspended in sterile PBS to an OD_{600}~1.0. 43816 and NTUH cultures were diluted 1:80,000 in sterile PBS to obtain the desired final concentration. Challenge doses of 43816 and NTUH were ~2000 CFU in 50 µL respectively. All other cultures were grown statically in LB broth for 16 h at 37 °C. Cultures were centrifuged at 8000 *x g* for 10 minutes, and pellets were resuspended in sterile PBS to an OD_{600}~1.0. Challenge doses for *cKp*120, KR174, and BEI669448 were ~10^8 CFU in 50 µL, respectively. BEI 702325 was further diluted 1:10 in sterile PBS for an infectious dose ~10^7 CFU in 50 µL. Mouse survival and weight were monitored daily for seven days. Mice were euthanized using CO_2 narcosis. Each experiment was performed in duplicate with $n = 10$ mice per group. Pairwise survival differences were determined by the Log-rank (Mantel-Cox) test. For the immunocompromised model, mice were treated with three separate IP injections of cyclophosphamide (CPM). The first injection was -4 days prior to infection at 150 mg/kg weight based on the average weight of all mice. The second and third injections are at days −2 before infection and day 2 after infection at 100 mg/kg weight based on the average weight of all mice. Bacteria were grown and prepared as stated above to an OD_{600}~1.0 then diluted to ~10^6 for BEI 702325 and *cKp*120, ~10^7 for KR174, and ~10^8 for BEI 669448. Mice were monitored for weight and survival daily for seven days. Each experiment was performed in duplicate with $n = 10$ mice per group. Pairwise survival differences were determined by the Log-rank (Mantel-Cox) test. All graphs and statistics were generated using GraphPad Prism version 10.

Data availability

Data related to this study is openly accessible at Digital Commons Data@Becker repository at Washington University School of Medicine (https://doi.org/10.17632/kzc9z43fyc).

Received: 19 July 2025; Accepted: 6 November 2025;
Published online: 13 December 2025

References

1. Bassat, Q. et al. Causes of Death Among Infants and Children in the Child Health and Mortality Prevention Surveillance (CHAMPS) Network. *JAMA Netw. Open* **6**, e2322494 (2023).
2. Munoz-Price, L. S. et al. Clinical epidemiology of the global expansion of Klebsiella pneumoniae carbapenemases. *Lancet Infect. Dis.* **13**, 785–796 (2013).
3. Chen, L. et al. Carbapenemase-producing Klebsiella pneumoniae: molecular and genetic decoding. *Trends Microbiol.* **22**, 686–696 (2014).
4. Kochan, T. J. et al. Genomic surveillance for multidrug-resistant or hypervirulent Klebsiella pneumoniae among United States bloodstream isolates. *BMC Infect. Dis.* **22**, 603 (2022).
5. Magill, S. S. et al. Changes in prevalence of health care-associated infections in U.S. Hospitals. *N. Engl. J. Med* **379**, 1732–1744 (2018).
6. Russo, T. A. & Marr, C. M. Hypervirulent Klebsiella pneumoniae. *Clin. Microbiol. Rev*. **32**, https://doi.org/10.1128/CMR.00001-19 (2019).
7. Zhao, Y. et al. An outbreak of Carbapenem-resistant and Hypervirulent. *Front Public Health* **7**, 229 (2019).
8. Kochan, T. J. et al. Klebsiella pneumoniae clinical isolates with features of both multidrug-resistance and hypervirulence have unexpectedly low virulence. *Nat. Commun.* **14**, 7962 (2023).
9. Goldblatt, D. Conjugate vaccines. *Clin. Exp. Immunol.* **119**, 1–3 (2000).
10. Wantuch, P. L. & Avci, F. Y. Current status and future directions of invasive pneumococcal diseases and prophylactic approaches to control them. *Hum. Vaccin Immunother.* **14**, 2303–2309 (2018).
11. Wyres, K. L. et al. Genomic surveillance for hypervirulence and multi-drug resistance in invasive Klebsiella pneumoniae from South and Southeast Asia. *Genome Med* **12**, 11 (2020).
12. Follador, R. et al. The diversity of Klebsiella pneumoniae surface polysaccharides. *Micro Genom.* **2**, e000073 (2016).
13. Shirley, M. 20-Valent Pneumococcal conjugate vaccine: a review of its use in adults. *Drugs* **82**, 989–999 (2022).
14. Shirley, M. 20-valent pneumococcal conjugate vaccine: pediatric first approval. *Paediatr. Drugs* **25**, 613–619 (2023).
15. Marr, C. M. & Russo, T. A. Hypervirulent Klebsiella pneumoniae: a new public health threat. *Expert Rev. Anti Infect. Ther.* **17**, 71–73 (2019).
16. Wyres, K. L. et al. Identification of Klebsiella capsule synthesis loci from whole genome data. *Micro Genom.* **2**, e000102 (2016).
17. Wantuch, P. L. et al. Capsular polysaccharide inhibits vaccine-induced O-antigen antibody binding and function across both classical and hypervirulent K2:O1 strains of Klebsiella pneumoniae. *PLoS Pathog.* **19**, e1011367 (2023).
18. Feldman, M. F. et al. A promising bioconjugate vaccine against hypervirulent Klebsiella pneumoniae. *Proc. Natl. Acad. Sci. USA* **116**, 18655–18663 (2019).
19. Lee, I. M. et al. A hexasaccharide from capsular polysaccharide of carbapenem-resistant Klebsiella pneumoniae KN2 is a ligand of Toll-like receptor 4. *Carbohydr. Polym.* **278**, 118944 (2022).

20. Kubler-Kielb, J. et al. The capsular polysaccharide and lipopolysaccharide structures of two carbapenem resistant Klebsiella pneumoniae outbreak isolates. *Carbohydr. Res.* **369**, 6–9 (2013).
21. Toh, Z. Q. et al. Evaluating functional immunity following encapsulated bacterial infection and vaccination. *Vaccines* **9**, https://doi.org/10.3390/vaccines9060677 (2021).
22. Paschall, A. V., Middleton, D. R. & Avci, F. Y. Opsonophagocytic killing assay to assess immunological responses against bacterial pathogens. *J. Vis. Exp.* https://doi.org/10.3791/59400 (2019).
23. Wantuch, P. L., Knoot, C. J., Marino, E. C., Harding, C. M. & Rosen, D. A. Klebsiella pneumoniae bioconjugate vaccine functional durability in mice. *Vaccine* **43**, 126536 (2025).
24. Tofas, P. et al. Carbapenemase-producing Klebsiella pneumoniae bloodstream infections in neutropenic patients with haematological malignancies or aplastic anaemia: Analysis of 50 cases. *Int J. Antimicrob. Agents* **47**, 335–339 (2016).
25. Gustinetti, G. & Mikulska, M. Bloodstream infections in neutropenic cancer patients: A practical update. *Virulence* **7**, 280–297 (2016).
26. Opota, O., Croxatto, A., Prod'hom, G. & Greub, G. Blood culture-based diagnosis of bacteraemia: state of the art. *Clin. Microbiol. Infect.* **21**, 313–322 (2015).
27. Wantuch, P. L. et al. A heptavalent O-antigen bioconjugate vaccine exhibits differential functional antibody responses against diverse Klebsiella pneumoniae isolates. *J. Infect. Dis.* https://doi.org/10.1093/infdis/jiae097 (2024).
28. Held, T. K., Jendrike, N. R., Rukavina, T., Podschun, R. & Trautmann, M. Binding to and opsonophagocytic activity of O-antigen-specific monoclonal antibodies against encapsulated and nonencapsulated Klebsiella pneumoniae serotype O1 strains. *Infect. Immun.* **68**, 2402–2409 (2000).
29. Williams, P., Lambert, P. A. & Brown, M. R. Penetration of immunoglobulins through the Klebsiella capsule and their effect on cell-surface hydrophobicity. *J. Med. Microbiol.* **26**, 29–35 (1988).
30. Mestas, J. & Hughes, C. C. Of mice and not men: differences between mouse and human immunology. *J. Immunol.* **172**, 2731–2738 (2004).
31. Budnick, J. A., Bina, X. R. & Bina, J. E. Complete Genome Sequence of Klebsiella pneumoniae Strain ATCC 43816. *Microbiol. Resour. Announc.* **10**, https://doi.org/10.1128/MRA.01441-20 (2021).
32. Wu, K. M. et al. Genome sequencing and comparative analysis of Klebsiella pneumoniae NTUH-K2044, a strain causing liver abscess and meningitis. *J. Bacteriol.* **191**, 4492–4501 (2009).
33. Martin, M. J. et al. A panel of diverse Klebsiella pneumoniae clinical isolates for research and development. *Microb. Genom.* **9**, https://doi.org/10.1099/mgen.0.000967 (2023).
34. Russo, T. A. et al. Identification of biomarkers for differentiation of hypervirulent Klebsiella pneumoniae from Classical K. pneumoniae. *J. Clin. Microbiol*. **56,** https://doi.org/10.1128/JCM.00776-18 (2018).
35. Datsenko, K. A. & Wanner, B. L. One-step inactivation of chromosomal genes in Escherichia coli K-12 using PCR products. *Proc. Natl. Acad. Sci. USA* **97**, 6640–6645 (2000).
36. Lee, D. J. et al. Gene doctoring: a method for recombineering in laboratory and pathogenic Escherichia coli strains. *BMC Microbiol.* **9**, 252 (2009).
37. CDC and FDA Antibiotic Resistance Isolate Bank. *Ceftolozane/tazobactam (CTV)*, https://wwwn.cdc.gov/ARIsolateBank/panel/PanelDetail?ID=4.
38. Pan, C. et al. Biosynthesis of conjugate vaccines using an O-linked glycosylation system. *mBio* **7**, e00443–00416 (2016).
39. Marty, M. T. et al. Bayesian deconvolution of mass and ion mobility spectra: from binary interactions to polydisperse ensembles. *Anal. Chem.* **87**, 4370–4376 (2015).
40. Caval, T., Zhu, J. & Heck, A. J. R. Simply extending the mass range in electron transfer higher energy collisional dissociation increases confidence in N-Glycopeptide identification. *Anal. Chem.* **91**, 10401–10406 (2019).
41. Rappsilber, J., Ishihama, Y. & Mann, M. Stop and go extraction tips for matrix-assisted laser desorption/ionization, nanoelectrospray, and LC/MS sample pretreatment in proteomics. *Anal. Chem.* **75**, 663–670 (2003).
42. Kong, A. T., Leprevost, F. V., Avtonomov, D. M., Mellacheruvu, D. & Nesvizhskii, A. I. MSFragger: ultrafast and comprehensive peptide identification in mass spectrometry-based proteomics. *Nat. Methods* **14**, 513–520 (2017).
43. Polasky, D. A., Yu, F., Teo, G. C. & Nesvizhskii, A. I. Fast and comprehensive N- and O-glycoproteomics analysis with MSFragger-Glyco. *Nat. Methods* **17**, 1125–1132 (2020).
44. Polasky, D. A., Geiszler, D. J., Yu, F. & Nesvizhskii, A. I. Multiattribute Glycan identification and FDR control for Glycoproteomics. *Mol. Cell Proteom.* **21**, 100205 (2022).
45. Brademan, D. R., Riley, N. M., Kwiecien, N. W. & Coon, J. J. Interactive peptide spectral annotator: a versatile web-based tool for proteomic applications. *Mol. Cell Proteom.* **18**, S193–S201 (2019).
46. Perez-Riverol, Y. et al. The PRIDE database at 20 years: 2025 update. *Nucleic Acids Res.* **53**, D543–D553 (2025).
47. Nahm, M. H., Briles, D. E. & Yu, X. Development of a multi-specificity opsonophagocytic killing assay. *Vaccine* **18**, 2768–2771 (2000).
48. Wagstaffe, H. R. et al. The development of immunological assays to evaluate the level and function of antibodies induced by Klebsiella pneumoniae O-antigen vaccines. *mSphere* **8**, e0068022. https://doi.org/10.1128/msphere.00680-22 (2023).

Acknowledgements

We would like to thank Dr. Thomas Russo for graciously providing us with cKp120 used in this study. This work was supported by the Washington University Department of Pediatrics and the National Institute of Allergy and Infectious Diseases: R01AI175038 (to DR), R41AI167078 (to CH), and R42AI165116 (to CH). The funders had no role in study design, data collection and analysis, decision to publish, or preparation of the manuscript.

Author contributions

P.L.W.: Conceptualization, Methodology, Validation, Investigation, Writing, Visualization. C.J.K., L.S.R., I.D., and A.M.M.: Methodology, Investigation. E.V.: Methodology, Validation, Investigation. N.E.S.: Methodology, Validation, Investigation. C.M.H.: Conceptualization, Methodology, Writing, Supervision. D.A.R.: Conceptualization, Methodology, Writing, Supervision. All authors have read and approved the manuscript.

Competing interests

LSR, CJK, ID, AMM, and CMH have a financial stake in Omniose, a for-profit entity developing bioconjugate vaccines using patented technology derived from the data presented in this and other published manuscripts. PLW, EV, NES, and DAR declare no competing interests.

Additional information

Supplementary information The online version contains supplementary material available at https://doi.org/10.1038/s41541-025-01314-7.

Correspondence and requests for materials should be addressed to David A. Rosen.